Indonesian Journal of Environmental Management and Sustainability
e-ISSN:2598-6279 *p*-ISSN:2598-6260

IJEMS

Research Paper

Utilizing *Areca catechu* L. Fruit Peel-Derived Biochar and Hydrochar for Congo Red Adsorption: Kinetic and Thermodynamic Analysis

Robiatul Adawiyah[1], Nova Yuliasari[2], Yulizah Hanifah[3], Kamila Alawiyah[4], Neza Rahayu Palapa[2*]

[1]*Master Program of Materials Science, Graduate School, Universitas Sriwijaya, Palembang, 30139, Indonesia*
[2]*Department of Chemistry, Faculty of Mathematics and Natural Sciences, Universitas Sriwijaya, Palembang, 30662, Indonesia*
[3]*National Research and Innovation Agency (BRIN), PUSPIPTEK, Tangerang Selatan, 15311, Indonesia*
[4]*Biology Department, Faculty of Mathematics and Natural Science, Universitas Sriwijaya, Palembang, 30662, Indonesia*
***Corresponding author e-mail**: nezarahayu@mipa.unsri.ac.id

Abstract
This study explores the conversion of *Areca* fruit peel into carbon-based materials biochar (BC) and hydrochar (HC) for use as adsorbents in synthetic dye removal from wastewater. Conversion was achieved through pyrolysis for BC and hydrothermal carbonization (HTC) for HC. X-ray diffraction (XRD) analysis confirmed carbon formation, with both HC and BC showing an amorphous characteristics. FTIR analysis identified hydroxyl, carboxyl, acid, and ester functional groups in BC, HC and *Areca* fruit peel materials that are essential for adsorption. BET surface area measurements showed 82.584 m^2/g for BC and 77.618 m^2/g for HC. Adsorption experiments demonstrated CR removal capacities of 40.515 mg/g for HC and 40.616 mg/g for BC, significantly surpassing the 23.168 mg/g capacity of untreated *Areca* fruit peel. Over three regeneration cycles, both BC and HC retained structural integrity, highlighting their potential as reusable adsorbents for dye removal. These results suggest that *Areca* fruit peel-derived BC and HC are promising, sustainable adsorbents for wastewater treatment, particularly in mitigating environmental impacts from industrial dyes.

Keywords
Biochar, Hydrochar, Biomass, Kinetics Adsorption and Thermodynamic Adsorption

Received: 7 August 2024, Accepted: 13 November 2024
https://doi.org/10.26554/ijems.2024.8.4.135-144

1. INTRODUCTION

Areca catechu L., commonly known as the *Areca* palm, is widely distributed across tropical and subtropical regions, especially Indonesia (Peng et al., 2015). This palm species offers a variety of benefits, with its fruit playing a significant cultural role in many Asian societies (Chao et al., 2020). The leaves of the *Areca* palm contain essential oils used in traditional medicine, the leaf sheaths are employed as food wrappers, the trunk serves as a building material, and the seeds have been traditionally used as a natural dye (Senthil Amudhan et al., 2012). Despite these varied uses, the peel of the *Areca* fruit remains underutilized, even though it contains a high cellulose content, approximately 57.35% by weight (Chao et al., 2020).

The cellulose-rich peel of the *Areca* fruit has significant potential for charcoal production, a carbon-rich residue obtained from renewable resources like *Areca* biomass. Charcoal, particularly in the form of biochar (BC) and hydrochar (HC), has gained considerable attention for its potential in various applications, including its use as an adsorbent (Kumar et al., 2020). BC is typically produced through pyrolysis of dry biomass, which requires high energy input due to the need for drying, making it more expensive for wet biomass (Sharma et al., 2022). To address the challenges associated with processing wet raw materials, researchers have turned to hydrothermal carbonization (HTC). HTC is a promising method for converting high-moisture biomass directly into hydrochar (HC) at relatively low temperatures (180–250°C), offering a more energy-efficient alternative (Mumme et al., 2011).

Hydrochar can be applied as solid fuel, for soil remediation, electron and hydrogen storage, toxic substances and heavy metal adsorption, carbon dioxide capture and storage, as well as dye adsorption (Tabassum et al., 2020). Biochar has been utilized for wastewater treatment (Chausali et al., 2021). Both biochar and hydrochar have been used to remove various pollutants from aqueous solutions, including organic compounds, metal ions, and certain dyes (Pauletto et al., 2021). Biochar as an adsorbent has offered many strength, such as being environmentally friendly, inexpen-

sive, easy to use, and available in abundant quantities for conversion into biochar. Additionally, biochar has shown potential for recycling and has exhibited a higher adsorption capacity compared to conventional adsorbents (Srivatsav et al., 2020). Both biochar and hydrochar have been utilized as adsorbents, with their high cellulose content contributing to the formation of biochar and hydrochar with large surface areas and microporous structures, making them highly effective as adsorbents (Mathew Tharayil and Chinnaiyan, 2023) Adsorbents have commonly been used for the adsorption of synthetic dye waste, largely due to the harmful effects of dye waste even at small amount of concentrations (Iqbal et al., 2021; Samaraweera et al., 2023). Congo Red is one of the industrial dyes frequently used in manufacturing sectors such as textiles, paper, and food processing. Industrial dye waste contributes approximately 20% of water pollution (Swan and Zaini, 2019). Consequently, water pollution resulting from dye discharge in industrial waste is hazardous, adversely affecting aquatic ecosystems, food chains, and public health. Therefore, low-cost and efficient waste reduction technologies are strongly recommended to mitigate these impacts on the ecosystem and public health (Palapa et al., 2023).

According to Hua et al. (2023) biochar derived from orange peels achieved an adsorption equilibrium time of 210 minutes and adsorpton capasity is 155.2 mg/g. Nitrogen-doped hydrochar was used to adsorb Congo red from water and adsorption capacity of 62.19 mg/g (Pauletto et al., 2021). Based on the research by Hammud et al. (2023), malachite green adsorption using activated biochar show an adsorption capacity of 62.80 mg/g, significantly higher than hydrochar, which had a capacity of 45.59 mg/g. The highest adsorption capacity reached 88% with a malachite green solution concentration of 66 ppm (Hammud et al., 2023). The adsorption capacity of Congo red on salak peel was 33.003 mg/g and the capacity increased to 133.333 mg/g when using hydrochar from salak peel (*Salacca zalacca*), according to Hasanah et al. (2022).

The selection of an appropriate adsorbent greatly influences the effectiveness and capacity of adsorption. The process typically involves the interaction between the adsorbent and adsorbate, the uptake of the adsorbate by the adsorbent, and the subsequent reuse of the adsorbent after the adsorption is complete. Biochar and hydrochar from *areca* fruit peel were selected due to the abundance of biomass waste and their structure, which consists of a large amount of cellulose (Al-Alwani et al., 2020).

This study aims to synthesize biochar and hydrochar from *Areca* catechu fruit peel in a simple, efficient process and to evaluate their effectiveness as adsorbents for removing congo red dye. Comprehensive characterization of the biochar is conducted to assess phase, functional groups, and morphology using XRD, FTIR, and BET analysis. Key factors influencing the adsorption process including temperature, contact time, and adsorbate concentration are analyzed to understand their impact on kinetic and thermodynamic parameters. Additionally, this research explores the regeneration capability of the biochar and hydrochar to assess their structural stability and potential for reuse, making them viable options for sustainable dye removal.

2. EXPERIMENTAL SECTION

2.1 Chemicals and Instrumentation

Materials used in this research include distilled water (H_2O) from PT. Dira Sonita, HCl, NaOH, NaCl, Congo red dye ($C_{32}H_{22}N_6Na_2O_6S_2$), and *Areca* fruit peel (*Areca catechu* L.) sourced from Pangandaran, West Java, Indonesia. Equipment utilized includes measuring cups, beakers, vacum, hotplate, funnel, filter paper, analytical balance, oven, magnetic stirrer, pH meter, thermometer, pipettes, centrifuge, hydrothermal stainless-steel autoclave, pyrolysis tool, XRD Rigaku Miniflex-6000, Quantachrome Micrometic ASAP and UV-Vis Biobase BK-UV 1800 PC spectrophotometer.

2.2 Preparation of *Areca* Fruit Peel

2.2.1 Preparation of Hydrochar from *Areca* Fruit Peel

The *Areca catechu* fruit peel was initially washed with distilled water to remove surface impurities, followed by sun-drying for 3 days to reduce its moisture content. Hydrochar was synthesized by adding 2.5 g of the *Areca* fruit peel to 50 mL of distilled water in a 100 mL hydrothermal stainless-steel autoclave, which was then heated at 250°C for 4 hours. Upon cooling, the resulting hydrochar was washed with distilled water to remove any residual substances, and subsequently dried in an oven at 105°C for 24 hours.

2.2.2 Preparation of Biochar from *Areca* Fruit Peel

The *Areca catechu* fruit peel was first rinsed with water to remove contaminants and then sun-dried for 3 days to reduce its moisture content. Following this, it was further dried in an oven at 80°C for 12 hours to eliminate any residual moisture and volatile compounds. After drying, the husk was pulverized into fine particles. The powdered material was then subjected to pyrolysis in a muffle furnace at 500°C under a constant nitrogen gas flow of 1×10^3 m^3/h for 3 hours. The resulting biochar was thoroughly washed and subsequently dried in a hot-air oven at 90°C for 12 hours (Bardalai and Mahanta, 2018).

2.3 Kinetcs Adsorption

The adsorption experiment using 0.02 g of *Areca catechu* fruit peel-based adsorbent biochar and hydrochar was added to a 100 mL Erlenmeyer flask containing 20 mL of dye solution at a concentration of 50 mg/L, without adjusting the pH of the dye. The mixture was agitated using a magnetic stirrer at time intervals of 10, 20, 30, 40, 50, 60, 90, 120, 150, and 180 minutes. After each stirring interval, the adsorbent and residual dye were separated through filtration, and the filtrate was collected. The absorbance of the filtrate was then

measured with a UV-Vis spectrophotometer. The adsorption kinetics were analyzed by plotting time against the dye adsorption process, with calculations based on Equations 1 and 2 (Normah et al., 2021).

$$log(Q_e - Q_t) = logQ_e – t \quad (1)$$

$$\frac{t}{Q_t} = \frac{1}{k_2 {Q_e}^2} + \frac{1}{Q_e} t \quad (2)$$

In this context, Q_e represents the equilibrium adsorption capacity (mg/g), while Q_t denotes the adsorption capacity at a given time (mg/g). The parameter t corresponds to the adsorption time in minutes. Additionally, k_1 is the rate constant for the pseudo-first-order (PFO) kinetic model (min^-), and k_2 represents the rate constant for the pseudo-second-order (PSO) kinetic model ($g.mg^{-1}.min^{-1}$).

2.4 Thermodynamic Adsorption

The thermodynamic effects on adsorption were investigated by varying both the dye concentration and adsorption temperature. In each experiment, 0.02 g of *Areca catechu* fruit peel, biochar and hydrochar were added to 20 mL of dye solution and stirred for 90 minutes using a magnetic stirrer. The experiments were conducted at different temperatures: 30, 40, 50, and 60°C. Following agitation, the mixture was filtered, and the absorbance of the filtrate was measured with a UV-Vis spectrophotometer. The adsorption capacity and adsorption energy were determined using Langmuir Equations 3 and 4, while the adsorption entropy and enthalpy were calculated using Equations 5 and 6 (Harja et al., 2022).

$$\frac{C_e}{Q_e} = \frac{C_e}{Q_m} + \frac{1}{Q_m k_L} \quad (3)$$

$$LogQ_e = logk_F + \frac{1}{n} logC_e \quad (4)$$

Where C_e represents the equilibrium concentration of the adsorbate (mg/L), Q_e denotes the adsorption capacity at equilibrium (mg/g), and Q_m is the maximum adsorption capacity (mg/g). The parameter k_L stands for the Langmuir constant (L/mg), while k_F is the Freundlich constant (mg/g).

$$ln\frac{Q_e}{Ce} = \frac{\Delta S}{R} - \frac{\Delta H}{RT} \quad (5)$$

$$\Delta G = \Delta H – T\Delta S \quad (6)$$

Where C_e represents the equilibrium concentration of the adsorbate (mg/L), and Q_e refers to the adsorption capacity at equilibrium (mg/g). The constant R is the ideal gas constant ($J/mol \cdot K$), and T denotes the temperature (K). The parameters ΔH, ΔS and ΔG represent the enthalpy change (kJ/mol), entropy change ($J/mol \cdot K$), and Gibbs free energy change (kJ/mol), respectively.

2.5 Regeneration

The regeneration process involved adding 0.2 g of *Areca catechu* fruit peel, biochar and hydrochar to 30 mL of 50 mg/L congo red dye solution. The mixture was stirred for 90 minutes, and the residual concentration of the dye measure using a UV-Vis spectrophotometer. After this, the adsorbent was dried and subjected to desorption using an ultrasonic device with 10 mL of water as the solvent, with stirring for an additional 90 minutes. The remaining residue was dried for reuse in the next regeneration cycle. The regeneration efficiency for Congo Red dye adsorption was calculated using Equation 7 (Palapa et al., 2021a).

$$\%\text{Regeneration} = \frac{Q_r}{Q_0} \times 100\% \quad (7)$$

Where Q_0 is initial adsorption capacity of the dye (mg/g) and Q_r is adsorption capacity of the dye after regeneration (mg/g).

3. RESULT AND DISCUSSION

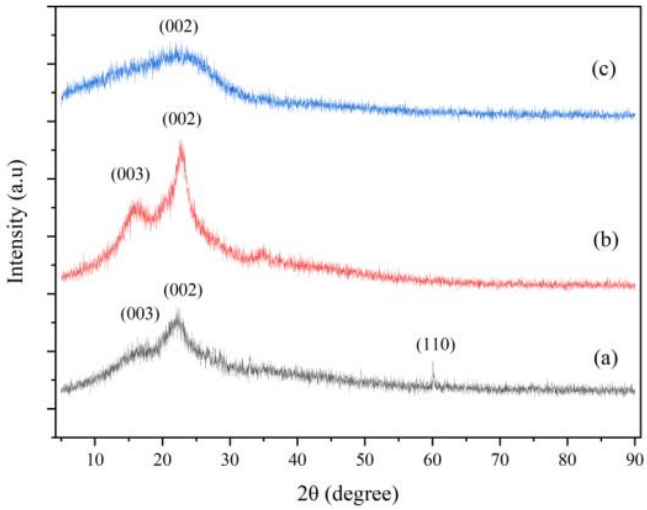

Figure 1. XRD Patern of (a) *Areca* Fruit Peel (b) HC (c) BC

The XRD diffractogram of *Areca* fruit peel Figure 1(a) reveals several peaks along with some noise, indicating the presence of multiple compounds. Significant peaks appear at 16.7° (003), 22.4° (002), and 60.77° (110), which suggests that *Areca* fruit peel exhibits amorf properties. In the case of hydrochar, as shown in Figure 1(b), peaks are observed at 22.96° (002) and 16.28° (003), which indicate the presence of amorphous characteristics. The peak intensities are higher than those observed for *Areca* fruit peel, suggesting a stronger amorphous structure in the hydrochar. Figure 1(c) displays a broad peak that suggests a high carbon content in the biochar, with diffraction occurring at 22.96° (002), indicating its largely amorphous structure. Biochar peaks at

Table 1. Kinetic Parameter

Adsorbent	Initial Concentration (mg/L)	Q_{eexp} (mg/g)	PFO			PSO		
			Q_{ecalc} (mg/g)	R^2	k_1	Q_{ecalc} (mg/g)	R^2	k_2
Areca fruit peel	51.583	23.168	11.902	0.807	-4.877	23.475	0.988	0.003
BC	52.175	40.515	11.517	0.748	-7.837	40.943	0.999	0.006
HC	52.656	40.644	13.513	0.850	-9.142	41.425	0.999	0.005

Table 2. Thermodynamic Adsorption

Adsorbent	Adsorption Isotherm	Adsorption Constant	T			
			30°C	40°C	50°C	60°C
Areca fruit peel	Langmuir	Q_{max}	384.615	112.360	84.746	68.493
		k_L	0.185	0.009	0.016	0.032
		R^2	0.002	0.8405	0.971	0.993
	Freundlich	k_F	0.707	1.571	2.532	4.859
		R^2	0.9822	0.973	0.978	0.963
		n	1.060	1.281	1.465	1.821
BC	Langmuir	Q_{max}	1435.506	286.413	138.847	112.370
		k_L	0.007	0.046	0.015	0.027
		R^2	0.018	0.056	0.296	0.611
	Freundlich	k_F	1.491	2.331	5.042	7.639
		R^2	0.821	0.813	0.810	0.871
		n	1.120	1.252	1.606	1.855
HC	Langmuir	Q_{max}	112.360	55.750	97.151	88.239
		k_L	0.013	0.030	0.036	0.061
		R^2	0.8405	0.875	0.871	0.944
	Freundlich	k_F	3.283	0.002	7.17	11.250
		R^2	0.973	0.942	0.944	0.968
		n	1.281	0.266	1.785	2.168

of 13.98 22.98 (60), 26.7 (39), and 43.0 (11). These results align with the findings of Bolbol et al. (2019), which describe biochar's diffraction pattern typically featuring a peak at (002), signifying its amorphous nature.

Areca catechu fruit peel, hydrochar, and biochar FT-IR spectrum is shown in Figure 2. The peak at 810 cm^{-1} corresponds to C–H bonds (Hua et al., 2023). Alkenes with C–H deformations were identified by peaks in the range of 850–790 cm^{-1}, while absorbance between 900–700 cm^{-1} suggests the presence of aromatic hydrocarbons. The absorbance peaks at 1110 cm^{-1} and 1019 cm^{-1} are associated with carbonyl-containing compounds, such as esters, ethers, alcohols, and acids (Khan et al., 2023). A band within 1650–1600 cm^{-1} signals C=C stretching vibrations, which may indicate non-conjugated dienes, or double-bonded hydrocarbons. Peaks for C=C bonds, indicative of aromatic hydrocarbons like benzene rings, are also present, providing additional stability to the material when applied (Kumar et al., 2020). Additionally, the presence of aromatic hydrocarbons in the *Areca catechu* biochar is suggested by small peaks around 1500 cm^{-1}. However, these aromatic hydrocarbon peaks were absent in the FTIR spectra of the *Areca catechu* biomass. Peaks within the range of 1500–2000 cm^{-1} are associated with the bending vibrations of absorbed H–O–H molecules. The FTIR analysis of the biochar revealed the presence of key functional groups, including hydroxyl, carboxyl, acid, and ester groups, which are notably abundant in both the synthesized biochar and hydrochar.

The mean pore diameters for biochar and hydrochar, measured via the Brunauer-Emmett-Teller (BET) method, were recorded at 1.539 nm and 1.521 nm, respectively. The BET analysis also revealed a surface area of 82.584 m^2/g for biochar and 77.618 m^2/g for hydrochar. These differences in surface characteristics likely stem from variations in the biomass source materials. With pore sizes within the mesoporous range, biochar and hydrochar exhibit structural properties characteristic of several types of activated carbon, which have proven effective in adsorbing Congo Red dye. Given the width of the Congo Red molecule, approximately 2.62 nm, a mesoporous architecture is essential for effective adsorption. Related studies, such as that by Gamboa et al. (2024), synthesized activated biochar from Haematoxylum

Table 3. Thermodynamic Adsorption

Adsorbent	T (K)	Q_e (mg/g)	ΔH (kJ/mol)	ΔS (J/mol K)	ΔG (kJ/mol)
Areca fruit peel	303	17.140	25.333	-0.078	51.902
	313	20.895			52.738
	323	23.754			53.574
	333	28.482			54.410
BC	303	19.947	20.826	-0.065	65.414
	313	21.807			66.502
	323	24.947			67.591
	333	29.184			68.679
HC	303	29.596	15.714	-0.055	62.013
	313	32.333			63.061
	323	33.439			64.109
	333	36.202			65.157

Table 4. Previous Study of CR Adsorption

Adsorbent	Kinetics Adsorption	Isotherm Adsorption	Adsoption Capacity (mg/g)	Refference
Amino grafted biochar (AMBC)	-	-	89.3	(Faheem et al., 2019)
Orange peel biochar	PSO	Langmuir	155.2	(Hua et al., 2023)
Algae-derived biochar	PSO	Langmuir	186.94	(Khan et al., 2023)
Biochar derived from waste pine needles	PSO	Langmuir	294.11	(Pandey et al., 2022)
Breadfruit Leaf Biochar	PSO	Langmuir	17.81	(Laxmi Deepak Bhatlu et al., 2023)
Activated Biochar from *Haematoxylum campechianum* Waste	-	Langmuir	114.8	(Gamboa et al., 2024)
The bamboo hydrochars	-	Freundlich	33.7	(Li et al., 2016)
Fly ash from a local power plant	PSO	Langmuir	22.12	(Harja et al., 2022)
Cellulose From Sago Frond	PSO	Langmuir	14.57	(Arnata et al., 2019))

campechianum waste with a mean pore diameter of 2.01 nm and a surface area of 124.15 m^2/g, successfully demonstrating Congo Red dye removal. The pore diameters and surface areas of biochar and hydrochar derived from *Areca* fruit peel show strong alignment with these findings, reinforcing their potential suitability for the adsorption of Congo Red from aqueous environments.

To investigate the influence of pH on the surface charge of *Areca* fruit peel, hydrochar (HC), and biochar (BC), we measured their surface potentials across different pH levels. As shown in Figure 2, the points of zero charge (PZC) for *Areca* fruit peel, HC, and BC were found to be 6.05, 6.08, and 7.08, respectively. These findings are consistent with Kumar et al. (2020) who reported that hydrochar tends to have a more acidic pH, while biochar is more alkaline. For *Areca* fruit peel, HC, and BC, the surface becomes positively charged at pH levels below 7.08, facilitating Congo red adsorption. However, as the pH rises above 7.08, the surface charge becomes increasingly negative, which reduces electrostatic attraction to Congo red, thereby diminishing the adsorption capacity. Therefore, in this study, the adsorption process was conducted without altering the native pH of congo red, which is 6.16.

In this study, the adsorption process was conducted using congo red's native pH of 6.16 to accurately mirror real-world conditions and minimize any interference that could result from pH adjustments. By preserving the natural pH, the inherent electrostatic interactions between the adsorbent surfaces (*Areca* fruit peel, hydrochar, and biochar) and congo red were maintained. At a pH of 6.16, the surface charge of the adsorbents is either near or just below their respective pH pzc values, especially for hydrochar and biochar, which enables optimal electrostatic attraction and enhances congo red adsorption. Additionally, avoiding pH modification prevents potential structural changes in the adsorbents, ensuring that the results represent the actual adsorption potential and environmental compatibility of these materials (Mathew Tharayil and Chinnaiyan, 2023).

Areca fruit peel, HC, and BC were used as adsorbents for removing Congo Red (CR). The kinetic parameters were

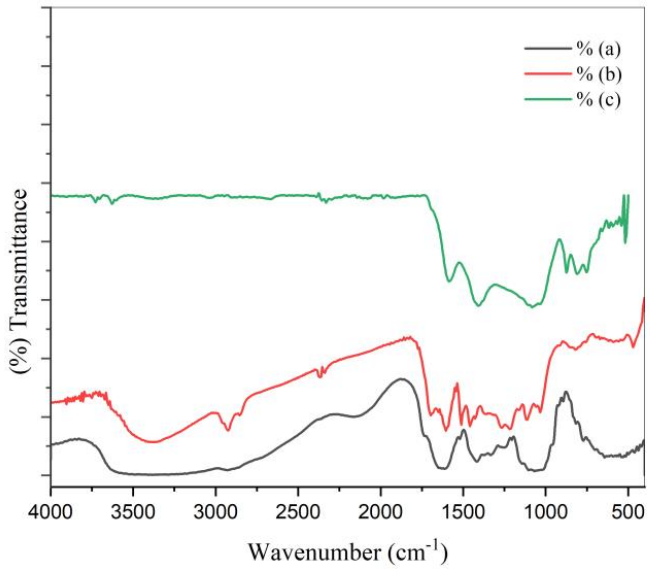

Figure 2. FT-IR Spectrum of (a) *Areca* Fruit Peel (b) HC (c) BC

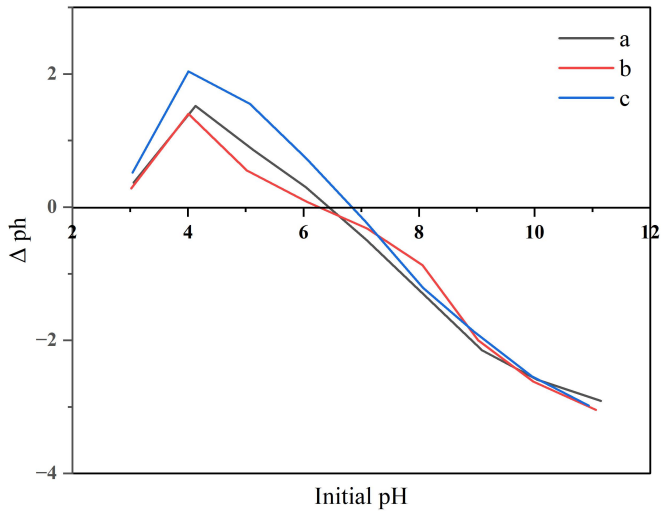

Figure 3. pHpzc Profile of *Areca* Fruit Peel (a) HC (b) and BC (c)

initially assessed by analyzing the impact of contact time on adsorption, utilizing Equation 1 and Equation 2, as illustrated in Figure 4 and summarized in Table 1. The data in Figure 4 show that equilibrium in CR adsorption was reached within 60 minutes. The adsorption process adheres to pseudo-second-order (PSO) kinetics, demonstrated by a correlation coefficient (R^2) close to unity. Additionally, the adsorption capacity (Q_e) predicted by the PSO model is in close agreement with the experimentally measured adsorption capacity (Q_e), as shown in Table 1.

In this study, the adsorption kinetics of Congo Red (CR) were examined using the pseudo-second-order (PSO)

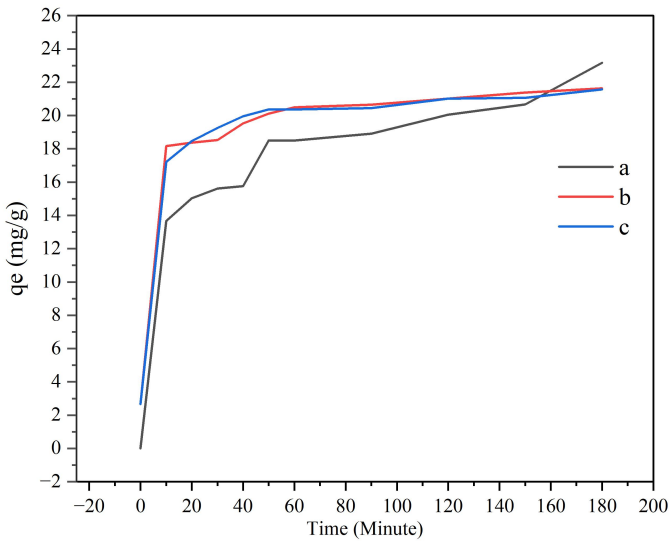

Figure 4. Kinetic Adsorption of CR of *Areca* Fruit Peel (a) HC (b) and BC (c)

model, which is based on the assumption that adsorption rate depends on the number of available adsorption sites and is primarily driven by chemisorption, involving electron sharing or exchange between the adsorbent and adsorbate (Pauletto et al., 2021). The high correlation coefficient (R^2), approaching unity, suggests that the PSO model effectively represents the kinetics of CR adsorption on *Areca* fruit peel, hydrochar (HC), and biochar (BC) (Hasanah et al., 2022). Furthermore, the close alignment between the predicted and observed adsorption capacities (Q_e) supports that the adsorption of CR on these materials is mainly governed by chemical interactions rather than physical forces. This model is therefore suitable for describing the adsorption process here, as it captures the significant role of chemical interactions between the adsorbate and the adsorbent surfaces, in line with the properties of congo red and the adsorbents used.

The adsorption mechanism involved in dye removal using has been analyzed through kinetic and isotherm models. Kinetic studies, including the pseudo-first-order and pseudo-second-order models, were performed to analyze the adsorption process. The pseudo-first-order model suggests that diffusion is the controlling factor, whereas the pseudo-second-order model attributes the process primarily to chemisorption mechanisms (Pandey et al., 2022). Figure 5 illustrate the results of these models, with Table 1 providing the derived kinetic parameters. The pseudo-second-order model exhibited a more linear fit, with an R^2 value greater than 0.998 for both HC and BC Adsorbent, indicating that the primary adsorption mechanism is surface diffusion and chemisorption (Srivatsav et al., 2020).

The interaction between CR and the *Areca* fruit peel, HC and BC surface was further analyzed using adsorption

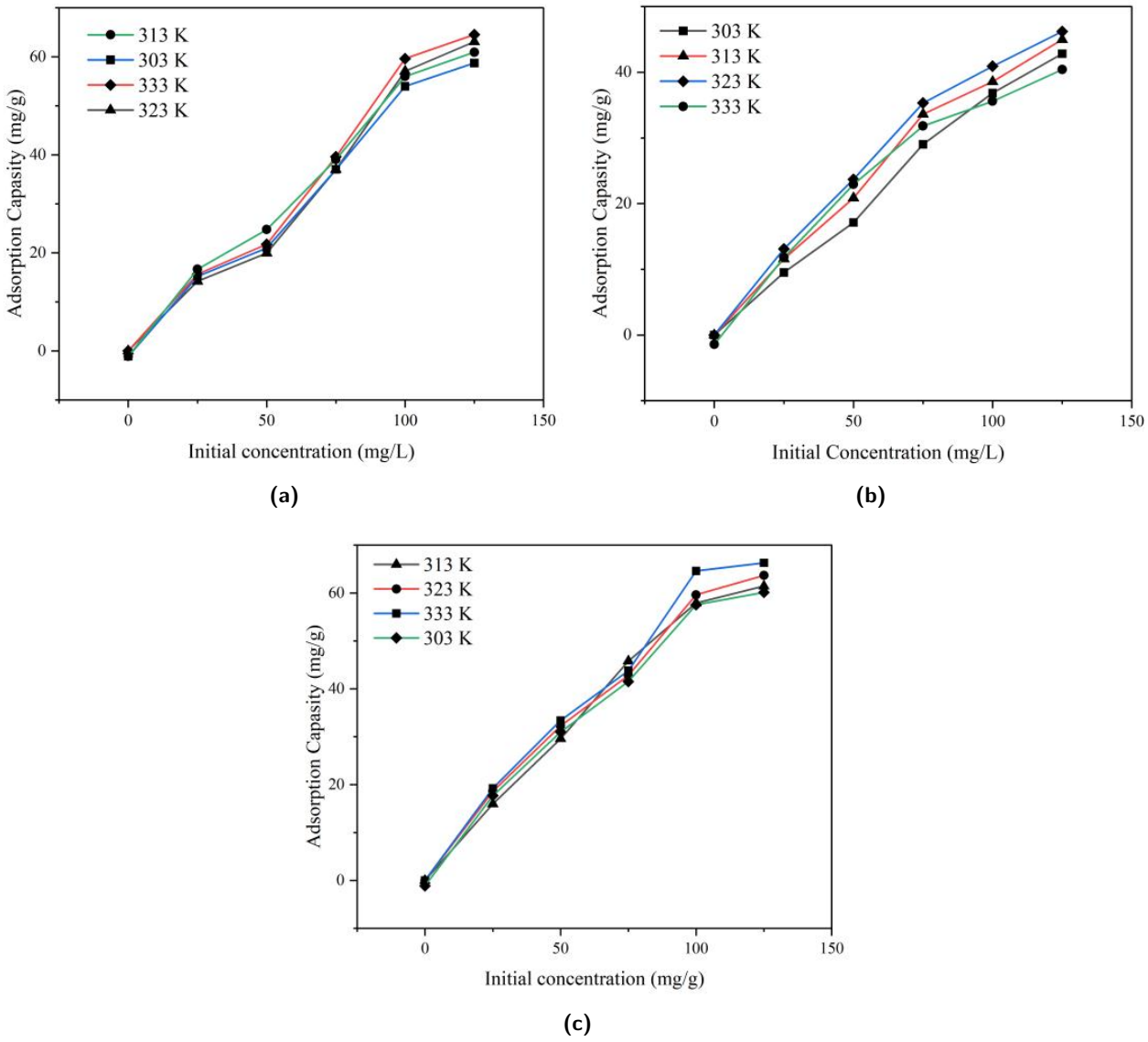

Figure 5. Effect Adsorption of Temprature on *Areca* Fruit Peel (a) HC (b) and BC (c)

isotherm studies, specifically the Langmuir and Freundlich models using Equation 3 and Equation 4 (Palapa et al., 2021b). Figure 5 and Table 2 display the results. The Fruedlich isotherm, which assumes multilayer adsorption with further adsorption beyond the superficial layer and uniform affinity across active sites, provided a better fit with an R^2 value of 0.998. This finding implies that the Freundlich model provides a better fit for the adsorption process compared to the Langmuir model (Hua et al., 2023). The maximum adsorption capacities (Q_m) calculated via the Langmuir model 23.168 mg/g for *Areca* fruit peel, 40.515 mg/g for HC, and 40.616 mg/g for BC align with experimental observations, reinforcing the suitability of the Freundlich model for this adsorption system. This result is in line with Table 4, which displays the adsorption of CR using a variety of adsorbents, and Table 4, which demonstrates that the majority of the adsorption isotherm mechanisms for Congo red are Langmuir isotherms. The adsorption capacity of CR in this study is fairly comparable to that found in other research.

The Freundlich isotherm, which assumes a heterogeneous adsorbent with multilayer adsorption and varying affinity, also provided valuable insights. The $1/n$ value, indicating the adsorbent's strength, was found to be greater than 1, which is considered acceptable and suggests the adsorbent's efficiency. The n value reflects the adsorbent's heterogeneous characteristics. This model is particularly applicable to materials such as hydrochar and biochar, where surface

heterogeneity is influenced by various structural and functional groups, likely due to the disrupted and fragmented carbon structures (Tabassum et al., 2020).

Gibbs free energy (ΔG) is an important thermodynamic indicator for determining the spontaneity of an adsorption process.Table 3 Display the values of ΔG is positive suggest that the adsorption process is non-spontaneous under the conditions applied. The enthalpy change (ΔH) represents the total heat energy exchanged during adsorption. A positive ΔH indicates that the process is endothermic, meaning that heat is absorbed from the surroundings into the system. The observation of a positive ΔH value suggests that Congo Red (CR) adsorption is endothermic, requiring energy input to occur (Wijaya et al., 2021).

The entropy change (ΔS) measures the level of disorder in the system. A negative ΔS value indicates that the system becomes more organized during adsorption. This suggests that as the dye concentration increases, the system's disorder decreases, likely due to more organized interactions between the adsorbent and CR. The negative ΔS value observed during the adsorption of CR indicates an increase in system order (Hasanah et al., 2022).

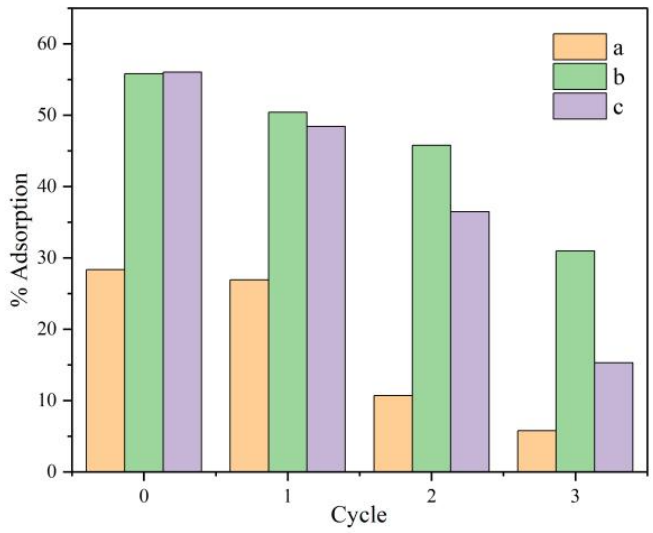

Figure 6. Regeneration of Adsorbent of *Areca* Fruit Peel (a) HC (b) and BC (c)

Figure 6 illustrates that hydrochar (HC) and biochar (BC) show more stable regeneration and higher adsorption capacities compared to raw *Areca* fruit peel. The re-adsorption rates for HC and BC, processed according to Equation 7, ranged from 56-15% over multiple cycles. Although the *Areca* fruit peel had a lower initial adsorption capacity, its re-adsorption capacity after three cycles, also analyzed with Equation 7, reached comparable values in the range of 28-6%. However, both HC and BC showed a decrease in adsorption capacity and structural stability over successive cycles, which is likely attributed to the breakdown of organic components caused by repeated adsorption-desorption processes. These findings suggest that converting *Areca* fruit peel into HC or BC enhances the structural stability and reusability of the adsorbent, providing a more robust material for Congo red removal in practical applications.

4. CONCLUSIONS

The conversion of *Areca* fruit peel into carbon-based materials, namely biochar and hydrochar, has been successfully achieved. XRD analysis confirms this, with a diffraction peak at $2\theta = 22°$ corresponding to the (002) plane, indicating the presence of carbon. Hydrochar exhibited a crystalline structure, while biochar displayed amorphous characteristics. FTIR analysis of the biochar revealed the presence of key functional groups, including hydroxyl, carboxyl, acid, and ester groups, which are highly evident in both the synthesized biochar and hydrochar. The surface area of the biochar, as determined by the Brunauer-Emmett-Teller (BET) method, was 82.584 m^2/g, while the hydrochar exhibited a surface area of 77.618 m^2/g. Both adsorbents proved effective in removing Congo red (CR), with adsorption capacities of approximately 23.168 mg/g for *Areca* fruit peel, 40.515 mg/g for hydrochar, and 40.616 mg/g for biochar. The regeneration process over three cycles showed that hydrochar and biochar retained their structural integrity, highlighting their potential as reusable adsorbents for CR removal.

5. ACKNOWLEDGEMENT

The authors express their gratitude to Universitas Sriwijaya for supporting this research through the SATEKS Unsri grant, number 0012/UN9/SK.LP2M.PT/2024. This article represents an additional contribution to the overall project. The authors would like to express their gratitude to the Research Center for Inorganic Materials and Complexes, FMIPA Universitas Sriwijaya, for their support in providing laboratory analysis. Additionally, the authors would like to thank the National Research and Innovation Agency (BRIN) for assisting in the pyrolysis process and material characterization.

REFERENCES

Al-Alwani, A., M. Hassimi, K. N. Al-Shorgani, and A. B. Abu (2020). Natural Dye Extracted from *Areca catechu* Fruits as a New Sensitiser for Dye-Sensitised Solar Cell Fabrication: Optimisation Using D-Optimal Design. *Materials Chemistry and Physics*, **240**; 122204

Arnata, I. W., S. Suprihatin, F. Fahma, N. Richana, and T. C. Sunarti (2019). Adsorption of Anionic Congo Red Dye by Using Cellulose From Sago Frond. *Pollution Research*, **38**(3); 43–53

Bardalai, M. and D. Mahanta (2018). Characterisation of Biochar Produced by Pyrolysis from *Areca catechu* Dust. *Materials Today: Proceedings*, **5**(1); 2089–2097

Bolbol, H., M. Fekri, and M. Hejazi-Mehrizi (2019). Layered Double Hydroxide–Loaded Biochar as a Sorbent for the Removal of Aquatic Phosphorus: Behavior and Mechanism Insights. *Arabian Journal of Geosciences*, **12**(16); 503

Chao, F.-L., T.-H. Yang, and J.-Y. Wu (2020). New Uses for *Areca catechu* Tree. *International Wood Products Journal*, **11**(2); 94–100

Chausali, N., J. Saxena, and R. Prasad (2021). Nanobiochar and Biochar Based Nanocomposites: Advances and Applications. *Journal of Agriculture and Food Research*, **5**; 100191

Faheem, J. Du, J. Bao, M. Hassan, S. Irshad, and M. Talib (2019). Multi-Functional Biochar Novel Surface Chemistry for Efficient Capture of Anionic Congo Red Dye: Behavior and Mechanism. *Arabian Journal for Science and Engineering*, **44**(12); 10127–10139

Gamboa, D., M. Abatal, E. Lima, F. Franseschi, C. Ucán, R. Tariq, M. Elías, and J. Vargas (2024). Sorption Behavior of Azo Dye Congo Red onto Activated Biochar from *Haematoxylum campechianum* Waste: Gradient Boosting Machine Learning-Assisted Bayesian Optimization for Improved Adsorption Process. *International Journal of Molecular Sciences*, **25**(9); 4771

Hammud, H. H., M. H. Hammoud, A. A. Hussein, Y. B. Fawaz, M. H. S. Abdul Hamid, and N. S. Sheikh (2023). Removal of Malachite Green Using Hydrochar From Palm Leaves. *Sustainability*, **15**(11); 8939

Harja, M., G. Buema, and D. Bucur (2022). Recent Advances in Removal of Congo Red Dye by Adsorption Using an Industrial Waste. *Scientific Reports*, **12**(1); 6087

Hasanah, M., A. Wijaya, F. Arsyad, R. Mohadi, and A. Lesbani (2022). Preparation of Hydrochar from *Salacca zalacca* Peels by Hydrothermal Carbonization: Study of Adsorption on Congo Red Dyes and Regeneration Ability. *Science and Technology Indonesia*, **7**(3); 372–378

Hua, Z., Y. Pan, and Q. Hong (2023). Adsorption of Congo Red Dye in Water by Orange Peel Biochar Modified with CTAB. *RSC Advances*, **13**(10); 6617–6626

Iqbal, J., N. S. Shah, M. Sayed, N. K. Niazi, M. Imran, J. A. Khan, Z. U. H. Khan, A. G. S. Hussien, K. Polychronopoulou, and F. Howari (2021). Nano-Zerovalent Manganese/Biochar Composite for the Adsorptive and Oxidative Removal of Congo-Red Dye from Aqueous Solutions. *Journal of Hazardous Materials*, **403**; 123854

Khan, A. A., S. R. Naqvi, I. Ali, W. Farooq, M. W. Anjum, H. AlMohamadi, S. S. Lam, M. Verma, H. S. Ng, and R. K. Liew (2023). Algal Biochar: A Natural Solution for the Removal of Congo Red Dye from Textile Wastewater. *Journal of the Taiwan Institute of Chemical Engineers*; 105312

Kumar, A., K. Saini, and T. Bhaskar (2020). *Hydrochar and Biochar: Production, Physicochemical Properties and Techno-Economic Analysis*, volume 310

Laxmi Deepak Bhatlu, M., P. S. Athira, N. Jayan, D. Barik, and M. S. Dennison (2023). Preparation of Breadfruit Leaf Biochar for the Application of Congo Red Dye Removal from Aqueous Solution and Optimization of Factors by RSM-BBD. *Adsorption Science & Technology*, **2023**; 7369027

Li, Y., A. Meas, S. Shan, R. Yang, and X. Gai (2016). Production and Optimization of Bamboo Hydrochars for Adsorption of Congo Red and 2-Naphthol. *Bioresource Technology*, **207**; 379–386

Mathew Tharayil, J. and P. Chinnaiyan (2023). Sustainable Waste Valorisation: Novel *Areca catechu* L. Husk Biochar for Anthraquinone Dye Adsorption - Characterization, Modelling, Kinetics, and Isotherm Studies. *Results in Engineering*, **20**; 101624

Mumme, J., L. Eckervogt, J. Pielert, M. Diakité, F. Rupp, and J. Kern (2011). Hydrothermal Carbonization of Anaerobically Digested Maize Silage. *Bioresource Technology*, **102**(19); 9255–9260

Normah, N. Juleanti, P. M. S. B. N. Siregar, A. Wijaya, N. R. Palapa, T. Taher, and A. Lesbani (2021). Size Selectivity of Anionic and Cationic Dyes Using LDH Modified Adsorbent with Low-Cost Rambutan Peel to Hydrochar. *Bulletin of Chemical Reaction Engineering & Catalysis*, **16**(4); 869–880

Palapa, N. R., N. Ahmad, H. P. Utami, Z. A. Zahara, R. Mohadi, and A. Lesbani (2023). Adsorption of Phenol Using Hydrochar Modified Layered Double Hydroxide – Kinetic, Isotherm, and Regeneration Studies. *Ecological Engineering and Environmental Technology*, **24**(5); 275–281

Palapa, N. R., T. Taher, N. Juleanti, Normah, and A. Lesbani (2021a). Biochar from Rice Husk as Efficient Biosorbent for Procion Red Removal from Aqueous Systems. *Applied Environmental Research*, **43**(3); 79–91

Palapa, N. R., T. Taher, A. Wijaya, and A. Lesbani (2021b). Modification of Cu/Cr Layered Double Hydroxide by Keggin Type Polyoxometalate as Adsorbent of Malachite Green from Aqueous Solution. *Science and Technology Indonesia*, **6**(3); 209–217

Pandey, D., A. Daverey, K. Dutta, and K. Arunachalam (2022). Enhanced Adsorption of Congo Red Dye onto Polyethyleneimine-Impregnated Biochar Derived from Pine Needles. *Environmental Monitoring and Assessment*, **194**(12); 880

Pauletto, P. S., J. Moreno-Pérez, L. E. Hernández-Hernández, A. Bonilla-Petriciolet, G. L. Dotto, and N. P. G. Salau (2021). Novel Biochar and Hydrochar for the Adsorption of 2-Nitrophenol from Aqueous Solutions: An Approach Using the PVSDM Model. *Chemosphere*, **269**; 128748

Peng, W., Y. Liu, N. Wu, T. Sun, X.-Y. He, Y.-X. Gao, and C.-J. Wu (2015). *Areca catechu* L. (Arecaceae): A Review of Its Traditional Uses, Botany, Phytochemistry, Pharmacology and Toxicology. *Journal of Ethnopharmacology*, **164**; 340–356

Samaraweera, V., S. Gunasekara, R. Nandasiri, A. Kumara,

D. Harischandra, K. Tennakoon, and N. Abidi (2023). Facile Preparation of Biochar Supported Nano-ZnO Photocatalyst for Efficient Adsorption and Degradation of Methylene Blue in Water. *Environmental Nanotechnology, Monitoring & Management*, **20**; 100792

Senthil Amudhan, M., H. Begum, and K. B. Hebbar (2012). A Review on Phytochemical and Pharmacological Potential of *Areca catechu* L. Seed. *IJPSR*, **3**(11); 4151–4157

Sharma, P. K., R. Kumar, R. K. Singh, P. Sharma, and A. Ghosh (2022). Review on Arsenic Removal Using Biochar-Based Materials. *Groundwater for Sustainable Development*, **17**; 100740

Srivatsav, P., B. S. Bhargav, V. Shanmugasundaram, J. Arun, K. P. Gopinath, and A. Bhatnagar (2020). Biochar As an Eco-Friendly and Economical Adsorbent for the Removal of Colorants (Dyes) from Aqueous Environment: A Review. *Water*, **12**(12); 3561

Swan, N. B. and M. A. A. Zaini (2019). Adsorption of Malachite Green and Congo Red Dyes from Water: Recent Progress and Future Outlook. *Ecological Chemistry and Engineering S*, **26**(1); 119–132

Tabassum, M., M. Bardhan, T. M. Novera, M. A. Islam, A. Hadi Jawad, and M. A. Islam (2020). NaOH-Activated Betel Nut Husk Hydrochar for Efficient Adsorption of Methylene Blue Dye. *Water, Air, & Soil Pollution*, **231**(8); 398

Wijaya, A., P. M. S. B. N. Siregar, A. Priambodo, N. R. Palapa, T. Taher, and A. Lesbani (2021). Innovative Modified of Cu-Al/C (C= Biochar, Graphite) Composites for Removal of Procion Red from Aqueous Solution. *Science and Technology Indonesia*, **6**(4); 228–234

